

# Bar Pullout Tests and Seismic Tests of Small-Headed Bars in Beam-Column Joints

by Thomas H.-K. Kang, Sang-Su Ha, and Dong-Uk Choi

*Experimental research was performed to evaluate the applicability of headed bars with small heads in exterior beam-column joints. A total of 12 pullout tests were first performed to examine anchorage behavior of headed bars subjected to monotonic and repeated loading, with test variables such as the head size, shape, and head-attaching technique. Reversed cyclic tests of two full-scale exterior beam-column joints were subsequently conducted to assess seismic performance. The pullout test results revealed that all types of heads and head-attaching techniques performed almost equally well, while the seismic test results indicated that the joint using small-headed bars showed better seismic performance than the joint using hooked bars in terms of damage extent, joint behavior, lateral drift capacity, and energy dissipation. In particular, the joint with headed bars generally satisfied ACI 374 acceptance criteria. These experimental results demonstrate that small-headed bars perform well with a development length shorter than that needed for hooked bars, and they can be effectively anchored in exterior beam-column joints under inelastic deformation reversals.*

**Keywords:** bar; cyclic loading; embedment length; joint; pullout; seismic.

## INTRODUCTION

In reinforced concrete structures, the use of 90-degree standard hooks is common where sufficient embedment depth is not available for developing straight bars. The development length in tension for standard hooks ( $l_{dh}$ ) ranges from only approximately 30 to 50% of that for straight bars ( $l_d$ ). The bends and tails of the hooked bars, however, tend to create reinforcing congestion, particularly in a region (for example, an exterior beam-column joint or knee joint) where all the beam and column main bars pass through or terminate. This congestion often hinders concrete placement and vibration inside a joint during casting. As a result, honeycombs (voids) can be produced, which are found after the forms are stripped.

The congestion problem gets worse with a relatively large amount of joint hoops and crossties. Time-consuming fabrication of congested reinforcement could be a serious concern for heavily reinforced members and joints. Potential solutions to reinforcing congestion problems include the use of: 1) headed deformed bars instead of hooked bars; 2) steel or high-performance fibers to reduce the amount of joint transverse reinforcement; and 3) self-consolidating concrete (which is not yet common in cast-in-place building construction in the U.S.). Simplified reinforcing detailing could save time and labor costs in construction. As such, headed reinforcement is quickly becoming a preferred means of anchorage and development of main reinforcing bars.

Despite the increased use of the headed reinforcement, there had been no design provisions dealing with headed bars until 2008. New design code provisions for the development length and details for headed bars have been added to ACI

318-08,<sup>1</sup> where the development length in tension for headed bars ( $l_{dt}$ ) is defined as

$$l_{dt} = \frac{0.19\psi_e f_y d_b}{\sqrt{f'_c}} \geq \text{the larger of } 8d_b \text{ and } 152 \text{ mm (6 in.)} \quad (1)$$

where  $f_y$  is the specified strength of headed bars in MPa;  $f'_c$  is the specified concrete strength in MPa;  $d_b$  is the bar diameter in mm;  $l_{dt}$  is in mm; and  $\psi_e = 1.2$  for epoxy-coated reinforcement and 1.0 for other cases. For psi units, the coefficient of 0.19 is replaced by 0.016. Equation (1) results in a development length of approximately 80% of that required for hooked bars by ACI 318-08.<sup>1</sup> A reduction factor of ( $A_s$  required)/( $A_s$  provided) may be applicable to Eq. (1). Although it has been observed that the head size influences anchorage capacity,<sup>2-4</sup> Eq. (1) is not a function of the head size. Rather, it is indirectly accounted for as one of the minimum requirements in ACI 318-08,<sup>1</sup> where acceptable criteria for material, geometrical, and reinforcing properties (for example, head size, clear cover, and spacing) are set forth. In this paper, “small head” is defined as a head with a ratio of ( $A_{brg}/A_b$ ) less than 4, while “large head” has a ratio of at least 4, where  $A_{brg}$  is the net bearing area of the head and  $A_b$  is the bar area.

For the design of headed bars in beam-column joints, ACI 352R-02,<sup>5</sup> “Recommendations for Design of Beam-Column Connections in Monolithic Reinforced Concrete Structures,” can be used, where the development length is defined as

$$l_{dt} = \frac{0.18f_y d_b}{\sqrt{f'_c}} \text{ for Type 1 joint} \quad (2)$$

$$l_{dt} = \frac{0.15f_y d_b}{\sqrt{f'_c}} \text{ for Type 2 joint} \quad (3)$$

In Eq. (3), a stress multiplier is already included to account for over-strength and strain-hardening of reinforcement (that is,  $\alpha = 1.25$ ). For psi units, the coefficients of 0.18 and 0.15 are replaced by 0.015 and 0.013, respectively. If the spacing of joint transverse reinforcement is less than or equal to  $3d_b$ , Eq. (2) is multiplied by 0.8. In ACI 352R-02,<sup>5</sup> a Type 2 joint is defined as a joint subjected to moderate-to-high seismic

ACI Structural Journal, V. 107, No. 1, January-February 2010.

MS No. S-2008-220.R1 received February 17, 2009, and reviewed under Institute publication policies. Copyright © 2010, American Concrete Institute. All rights reserved, including the making of copies unless permission is obtained from the copyright proprietors. Pertinent discussion including author's closure, if any, will be published in the November-December 2010 ACI Structural Journal if the discussion is received by July 1, 2010.

ACI member **Thomas H.-K. Kang** is an Assistant Professor of civil engineering at the University of Oklahoma, Norman, OK. He is Secretary of Joint ACI-ASCE Committee 352, Joints and Connections in Monolithic Concrete Structures, and is a member of ACI Committee 369, Seismic Repair and Rehabilitation; Joint ACI-ASCE Committee 423, Prestressed Concrete; E803, Faculty Network Coordinating Committee; and the ACI Collegiate Concrete Council. He received the ACI Wason Medal for Most Meritorious Paper in 2009. His research interests include seismic design and rehabilitation of concrete joints, connections and systems, and the behavior of new materials combined with concrete.

**Sang-Su Ha** is a full-time Lecturer of architectural engineering at Kangnam University, Yongin, Korea. He received his PhD from Hanyang University, Seoul, Korea. His research interests include experimental techniques of reinforced concrete structures, seismic tests of beam-column and slab-column connections, and the use of headed and fiber-reinforced polymer bars for anchorage and splicing.

ACI member **Dong-Uk Choi** is a Professor of architectural engineering at Hankyong National University, Ansong, Korea. He received his PhD from the University of Texas at Austin, Austin, TX. He is a member of ACI Committee 59-06, International Partnerships. His research interests include development and splicing of reinforcing bars, mechanical anchorage, and the behavior of concrete-to-concrete interfaces subjected to mechanical and thermal loading.

risks, whereas a Type 1 joint is defined as a joint subjected to low seismic risk. The development length ( $l_{dt}$ ) given by Eq. (2) is taken as 75% of  $l_{dh}$  of ACI 352R-02,<sup>5</sup> yielding approximately 80% of that ( $l_{dt}$ ) given by Eq. (1), where  $l_{dh}$  is the development length in tension for hooked bars. Equation (2) was developed based on various test results,<sup>2,6,7</sup> and was targeted toward the special case of beam-column joints. The shorter development length of Eq. (2) versus Eq. (1) appears to be based on the fact that headed bars are anchored in the diagonal strut of a well-confined joint.<sup>8</sup> Additionally, column transverse reinforcement above the joint plays a role in preventing brittle concrete breakout as depicted in Fig. 1(a) (versus Fig. 1(b)).

To relieve steel congestion within the joint while promoting proper bearing, use of a circular head with ( $A_{brg}/A_b$ ) of approximately 4 is common. Prior experimental research<sup>4,7,8</sup> has shown that this head size is appropriate to ensure anchorage both in the elastic and inelastic deformation ranges, and a minimum ratio of ( $A_{brg}/A_b$ ) = 4 is specified by ACI 318-08.<sup>1</sup> The head size standard of ( $A_{brg}/A_b$ ) = 4 is relatively easy to maintain in practice. The size of ( $A_{brg}/A_b$ ) = 9 was originally recommended by the previous 1998 version of ASTM A970,<sup>9</sup> which is often impractical; for this reason, the specification that requires ( $A_{brg}/A_b$ ) of at least 9 no longer exists in ASTM A970-04.<sup>10</sup>

In this study (which was planned when no clear design provisions of the headed bars existed), the head size was investigated as one of the main research variables to provide design guidelines for the use of headed bars. Both circular and square head shapes were examined to observe the impact of head shape on anchorage response. Along with two prior companion experimental studies<sup>11,12</sup> where several parameters affecting anchorage strength were investigated, an attempt was made to find a quantitative answer to the question of which combination of development length and head size might be appropriate for the design of beam-column joints. Based on the previous results<sup>11,12</sup> and present pullout test results, a set of development length and head size was selected for seismic testing and evaluation of a beam-column joint subassembly with headed bars. Another subassembly with the same configuration, except for the use of hooked bars, was also evaluated for comparison. This study aimed to test the general applicability of headed bars with small heads in exterior beam-column joints. Results of the study were then compared with the ACI 318-08<sup>1</sup> headed bar provisions, which have been recently stipulated.

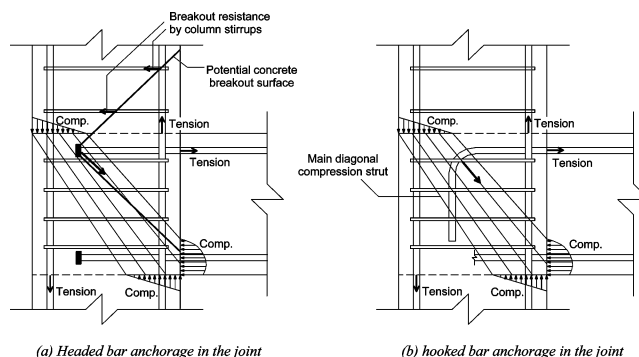


Fig. 1—Forces: (a) and (b) resulting in diagonal compression struts; and (a) in column above joint.

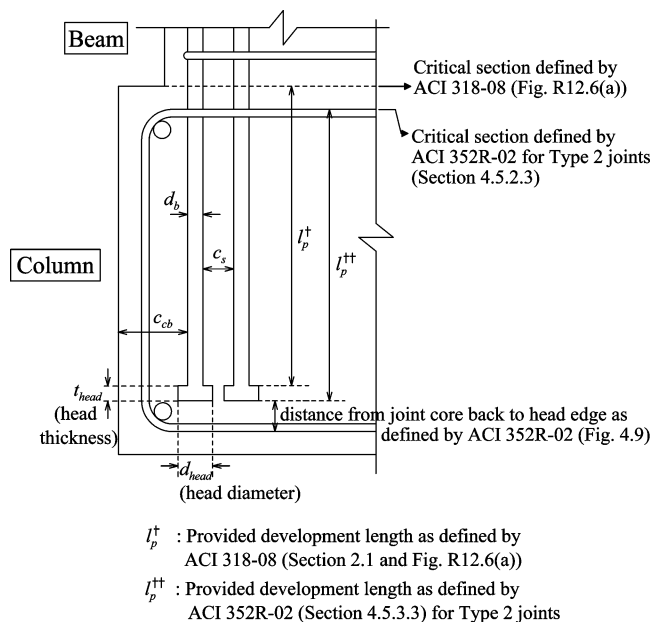


Fig. 2—Definitions of development lengths, critical sections, and head details.

## RESEARCH SIGNIFICANCE

An experimental study was devised to assess pullout and seismic anchorage behavior of headed bars with small heads. The small head size used ( $A_{brg}/A_b = 2.7$ ) substantially relieves reinforcing congestion and helps minimize column bar obstruction when inserting a beam reinforcing cage into the column cage. This is an important constructibility aspect. A total of 12 pullout specimens and two full-scale reinforced concrete beam-column joint subassemblies were tested to observe the influence of head size, shape, and head-attaching techniques on anchorage capacity and evaluate the seismic performance of exterior beam-column joints with small-headed bars.

## SUMMARY OF PRIOR COMPANION EXPERIMENTAL RESEARCH

Choi<sup>11</sup> and Choi et al.<sup>12</sup> conducted a total of 80 pullout tests to investigate the anchorage behavior of single and multiple headed bars embedded in well-confined concrete. A square head, a head thickness ( $t_{head}$ ; refer to Fig. 2) of  $1d_b$ , and a uniform head size of ( $A_{brg}/A_b$ )  $\approx 3$  were used for all tests. The following is a summary of the test results.

1. Anchorage strengths for both hooked and single headed bars ranged from 112 to 125% of the design bar yield

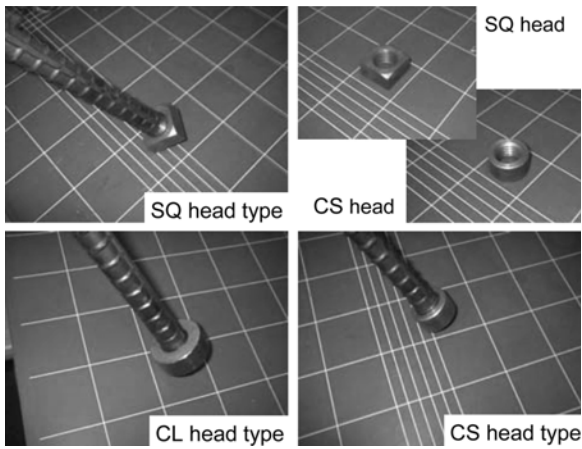


Fig. 3—Head types (refer to Table 1 for definitions).

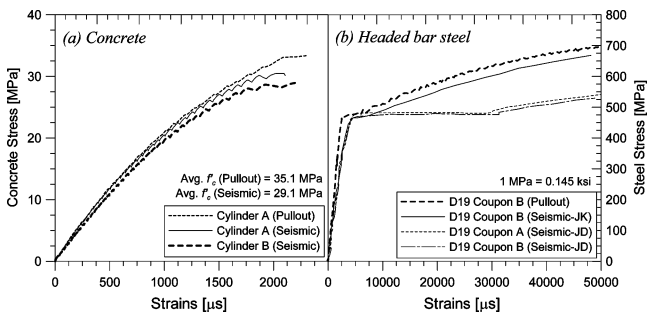


Fig. 4—Stress-strain relations for materials.

strengths, provided that embedment depth  $h_d$  was only  $10d_b$  ( $0.12f_{y,meas} d_b / \sqrt{f'_{c,meas}}$ ) and side cover to the bar ( $c_{cb}$ ; refer to Fig. 2) was at least  $2.8d_b$ . Here,  $f_{y,meas}$  and  $f'_{c,meas}$  are assumed material properties of  $f_y$  and  $f'_c$ , respectively.

2. At least  $h_d$  of  $13d_b$  ( $0.18f_{y,meas} d_b / \sqrt{f'_{c,meas}}$ ) should be provided for a group of multiple headed bars to develop 125% of the design yield strengths, provided that  $c_{cb}$  was at least  $3.5d_b$  and adequate amount of confining transverse reinforcement was used (that is, steel-to-concrete volume ratio  $\geq 0.6\%$ ).

3. The range of clear bar spacing tested ( $c_s = 3.5d_b$  to  $8d_b$ ; refer to Fig. 2) did not affect the anchorage behavior of multiple headed bars.

4. As the side cover  $c_{cb}$  increased, the anchorage strength increased.

## EXPERIMENTAL PROGRAM

Based on the results of the prior experimental studies presented in the preceding section, an embedment length of  $10d_b$  ( $0.13f_{y,meas} d_b / \sqrt{f'_{c,meas}}$ ) was used for new pullout tests of single headed bars, and  $15d_b$  ( $0.17f_{y,meas} d_b / \sqrt{f'_{c,meas}}$ ) was used for seismic tests of beam-column joints with multiple headed bars. This section presents an overview of the experimental program that examines the effect of head size, head shape, and head-attaching technique on the anchorage strength rather than the development length itself, and investigates the seismic behavior of headed bars anchored in exterior beam-column joints.

## Materials

Headed deformed bars with a bar diameter of 19 mm (D19) were used in this study. Three types of head

Table 1—Dimensions for heads and headed bars

ID	$d_b$ , mm (in.)	$A_b$ , mm <sup>2</sup> (in. <sup>2</sup> )	$d_{head}$ , mm (in.)	$t_{head}$ , mm (in.)	$A_{nh} \approx A_{brg}$ , mm <sup>2</sup> (in. <sup>2</sup> )	$A_{brg}/A_b$
SQ	19 (0.75)	284 (0.44)	NA	19 (0.75)	792 (1.23)	2.8
CL	19 (0.75)	284 (0.44)	46 (1.8)	19 (0.75)	1358 (2.10)	4.5
CS	19 (0.75)	284 (0.44)	36 (1.4)	19 (0.75)	730 (1.13)	2.6
NH	19 (0.75)	284 (0.44)	NA	NA	NA	0.0

Note: SQ is square; CL is circular large; CS is circular small; NH is no head;  $d_b$  is bar diameter (refer to Fig. 2);  $A_b$  is bar area;  $d_{head}$  is head diameter (refer to Fig. 2);  $t_{head}$  is head thickness (refer to Fig. 2);  $A_{nh}$  is net head area;  $A_{brg}$  is net bearing area of head; and NA is not available. In this study  $A_{brg} \approx A_{nh}$ , as there is little obstruction (per ACI 318-08, Section 3.5.9).<sup>1</sup>

Table 2—Measured steel material properties

	$d_b$ , mm (in.)	$E_s$ , GPa (ksi)	$f_{y,meas}$ , MPa (ksi)	$\epsilon_{y,meas}$	$f_{u,meas}$ , MPa (ksi)
D10	10 (0.4)	204 (29,580)	570 (83)	0.0028	697 (101)
D19-Pullout	19 (0.75)	181 (26,245)	465 (67)	0.0026	721 (105)
D19-JD	19 (0.75)	200 (29,000)	481 (70)	0.0024	575 (83)
D19-JK	19 (0.75)	200 (29,000)	460 (67)	0.0023	580 (84)
D25	25 (1.0)	204 (29,580)	407 (59)	0.0020	602 (87)

Note: Two steel coupons were tested and averaged for each bar size.  $E_s$  is measured modulus of elasticity;  $f_{y,meas}$  is measured yield stress;  $\epsilon_{y,meas}$  is measured strain at  $f_{y,meas}$ ; and  $f_{u,meas}$  is measured ultimate tensile stress.

geometries used for pullout tests are detailed in Table 1 and shown in Fig. 3. For reversed cyclic tests of the beam-column joint, small circular heads (CS; refer to Table 1) were chosen based on the pullout test results. All headed bars and heads were made of steel with a specified yield stress  $f_y$  of 400 MPa (58 ksi). The specified concrete strength was 27 MPa (4 ksi).

Measured material properties of steel and concrete are summarized in Table 2. Headed and hooked bars used for seismic tests had similar actual yield strengths of  $1.2f_y$  and  $1.15f_y$ , respectively, where  $f_y$  is the specified yield strength of 400 MPa (58 ksi). Different concrete mixes were used for pullout and seismic tests. For each test, two and three concrete cylinders were tested and averaged, respectively. Stress-strain relations were obtained for all 100 x 200 mm (4 x 8 in.) concrete cylinders and steel coupons with a length of 450 mm (18 in.) (Fig. 4).

## Pullout tests of single headed bars

In the pullout study, the same embedment depth  $h_d$  of  $10d_b$  (190 mm [7.5 in.]) was used for all tests to examine various parameters such as head types, head-attaching techniques (welding versus threading), and loading conditions (monotonic versus repeated). Two straight bars with an  $h_d$  of  $15d_b$  (no heads) were also tested for comparison. Table 3 summarizes the parameters tested. The ASTM A970<sup>10</sup> standard has permitted use of the threaded head-to-bar connection since 2004, in addition to the welded or forged head-to-bar connections, and the ACI 318-08<sup>1</sup> code (Section 3.5.9) refers to ASTM A970-04.<sup>10</sup> Thus, the head-attaching technique was selected as one of the test parameters to verify the ASTM standard.

For four of the 12 specimens, loading and unloading in tension were repeated three times for each stress level of 0.25, 0.5, 0.75, 1.0, and  $1.25f_{y,meas}$ , where  $f_{y,meas}$  is the measured yield stress of steel (465 MPa [67 ksi]). This was done to analyze the difference in anchorage behavior under different loading conditions. Subsequent to the repeated

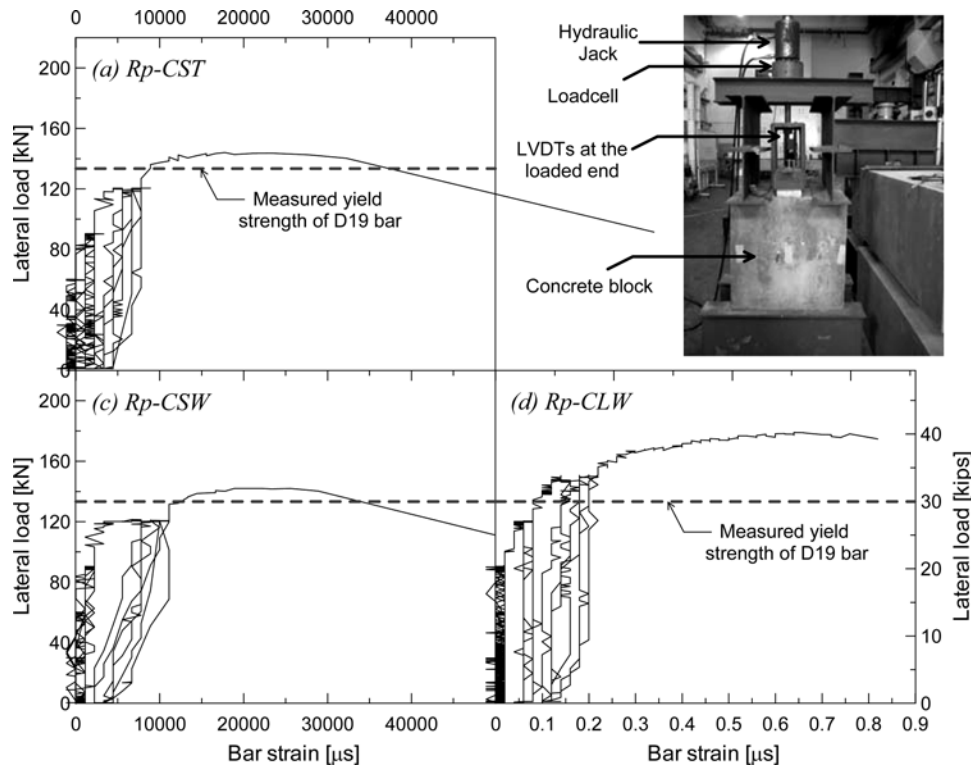


Fig. 5—Load-bar slip relations for repeated pullout tests.

Table 3—Summary of test parameters and results for pullout tests

ID	Loading type	Head type	Head attachment	$f'_{c, meas}$ , MPa (psi)	$h_d$ , mm (in.)	$L_{peak}$ , kN (kips)	$L_{peak}/(A_s f_{y, meas})$
Mnt-CST	Monotonic	CS	Threading	35.1 (5090)	190 (7.5)	165 (37)	1.13
Mnt-CLT	Monotonic	CL	Threading	35.1 (5090)	190 (7.5)	171 (38)	1.28
Mnt-SQT	Monotonic	SQ	Threading	35.1 (5090)	190 (7.5)	163 (37)	1.18
Mnt-CSW	Monotonic	CS	Welding	35.1 (5090)	190 (7.5)	148 (33)	1.11
Mnt-CLW	Monotonic	CL	Welding	35.1 (5090)	190 (7.5)	196 (44)	1.47
Mnt-SQW	Monotonic	SQ	Welding	35.1 (5090)	190 (7.5)	152 (34)	1.14
Mnt-NH1	Monotonic	NA	NA	35.1 (5090)	285 (11.2)	115 (26)	0.86
Mnt-NH2	Monotonic	NA	NA	35.1 (5090)	285 (11.2)	104 (23)	0.78
Rp-CST	Repeated	CS	Threading	35.1 (5090)	190 (7.5)	144 (32)	1.08
Rp-CLT	Repeated	CL	Threading	35.1 (5090)	190 (7.5)	181 (41)	1.35
Rp-CSW	Repeated	CS	Welding	35.1 (5090)	190 (7.5)	142 (32)	1.06
Rp-CLW	Repeated	CL	Welding	35.1 (5090)	190 (7.5)	179 (40)	1.34

Note:  $f'_{c, meas}$  is measured concrete strength;  $h_d$  is embedment depth measured from concrete surface to bearing face of head;  $L_{peak}$  is peak pullout load monitored;  $f_{y, meas}$  is measured yield stress of steel; and NA is not available.

loading steps, monotonic pullout loading was applied until loss of pullout load capacity.

Each specimen consisted of a single headed bar embedded at the center in a plain concrete block with dimensions of 700 x 700 x 700 mm (28 x 28 x 28 in.). Although the stem of a headed bar and the web of steel I-beams used as supports for a hydraulic jack were separated by at least 1.5 times the headed bar embedment depth in all tests, the bars were fairly confined by the reaction forces at the loaded end (refer to Fig. 5); however, because the degree of concrete confinement produced by such test configuration was not close enough to that in the beam-column joint, the pullout results were just used to make a preliminary decision for the selection of key headed bar parameters (for example, head size and head-to-bar connection) for joint subassembly tests. The current pullout tests were also appropriately used to make direct

comparisons for the aforementioned parameters under the same conditions.

The headed bar was subjected to tension using a hydraulic jack with a capacity of 500 kN (112 kips) (Fig. 5). A load cell was located under the jack to record the tension force. The head slips at the back of the head and at the loaded end were measured using linear variable displacement transducers (LVDTs). To attach the LVDT to the head, a 5 mm (0.2 in.) diameter steel rod was welded to the back surface of the head. The rod was then inserted inside the polyvinyl chloride (PVC) tube, which was embedded in the concrete prior to casting. Two strain gauges were mounted on each headed bar at the location of 50 mm (2 in.) away from the concrete surface (in the air) at the loaded end. All data were collected every 1 second with the data logger.

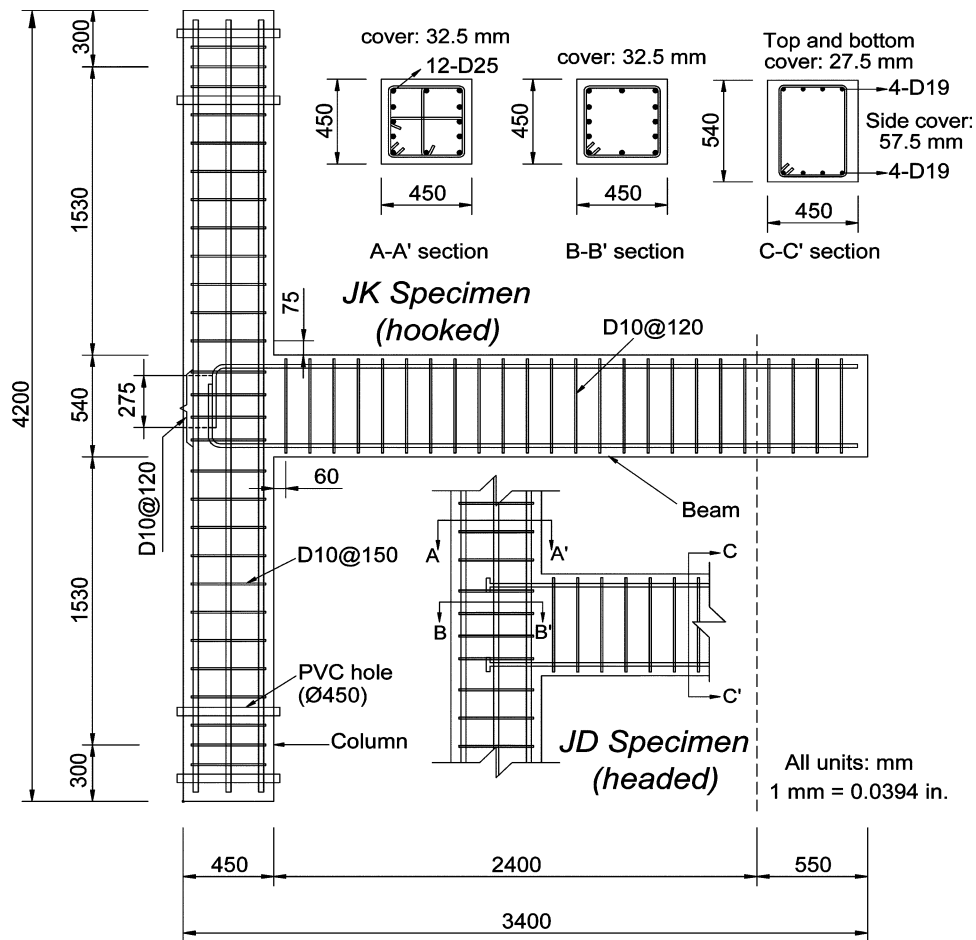


Fig. 6—Dimensions and details for JD and JK specimens.

### Reversed cyclic tests of beam-column joints

To evaluate the application of headed bars with small heads in exterior beam-column joints as compared to hooked bars, cyclic subassembly tests were conducted. Two full-scale joint subassemblies were constructed: one of headed bars (JD) and the other of 90-degree hooked bars (JK). As detailed in Fig. 6, the story height (3.6 m [142 in.]), center-to-center span length (5.25 m [207 in.]), and column and beam size and reinforcement were determined to correspond to typical actual dimensions of moment resisting frames. The same bar size (D19) used in pullout tests, conducted as part of this study, was also used in seismic tests. The small head size ( $A_{brg}/A_b = 2.6$ ), circular head shape, and threaded head-to-bar connection were chosen based on the observations from the pullout tests conducted herein, as well as the prior companion tests.<sup>11,12</sup>

**Development length**—The development length  $l_p$  provided for the JD specimen (headed) is 285 mm (11.25 in.) ( $15d_b$  or  $0.17f_{y, meas} d_b / \sqrt{f'_{c, meas}}$ ), measured from the beam-joint interface to the bearing face of the head. For the JK specimen (hooked),  $l_p$  is also 285 mm (11.25 in.) ( $15d_b$  or  $0.18f_{y, meas} d_b / \sqrt{f'_{c, meas}}$ ), measured from the interface to the outside edge of the hook. The development length used for JD is similar to that ( $0.18f_{y, meas} d_b / \sqrt{f'_{c, meas}}$ ) needed to develop  $1.25f_y$  of multiple headed bars in the prior pullout tests<sup>11</sup> or ( $l_{dt} = 0.19f_y d_b / \sqrt{f'_{c, meas}}$ ) required by the new headed bar provision of ACI 318-08<sup>1</sup> (Section 12.6.1).

For beam-column joints as part of a lateral-force-resisting system that is expected to deform in the inelastic range

(Type 2 joints), the critical section is considered to be located at the edge of the joint core (outside of joint hoop), according to Chapter 21 of ACI 318-08<sup>1</sup> and ACI 352R-02<sup>5</sup> (refer to Fig. 2). Also, it should be noted that the definitions of  $l_{dt}$  are different in ACI 318-08<sup>1</sup> and 352R-02.<sup>5</sup> The former defines  $l_{dt}$  as the length measured from the critical section to the “bearing face” of the head, whereas the latter is defined as the length to the “outside end” of the head (refer to Fig. 2). Table 4 summarizes the provided and required development lengths for beam bars used for the specimens. The definition of ACI 318-08<sup>1</sup> is used throughout the remainder of the paper.

The location of the head and hook extension did not exactly comply with ACI 352R-02<sup>5</sup> recommendations (Section 4.5.2.1) or ACI 318-08<sup>1</sup> commentary (R12.6). The outside edges of the head and the hook were located at 114 and 133 mm (4.5 and 5.25 in.), respectively, from the back of the joint core, versus the recommended location of 50 mm (2 in.) regarded as being in the diagonal compression zone by ACI 352R-02<sup>5</sup> (refer to Fig. 1 and 2). In this study, however, an attempt was made to provide the exact development length of  $15d_b$ , which often happens in actual practice, rather than meeting ACI 352R-02<sup>5</sup> (Section 4.5.2.1). Also, as a result of this configuration,  $l_p$  is smaller than  $l_{dh}$  for JK, where  $l_{dh}$  is the development length for a hooked bar. The current testing, however, gives an idea of the potential impact of this detail on joint behavior. Note that the 2008 version of ACI 318<sup>1</sup> began to explicitly state that the headed bar should extend to the far side of the joint core (Commentary R12.6 and Fig. R12.6(b)). Similar commentary is still not available for



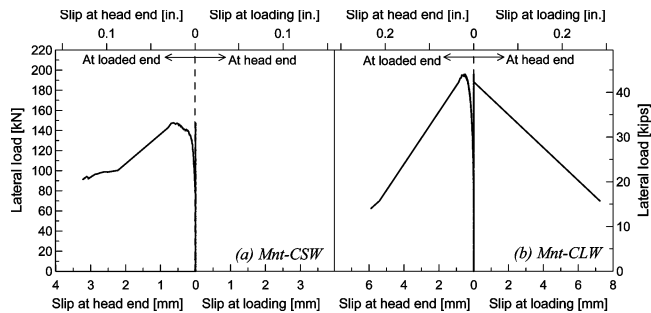


Fig. 9—Comparisons between slips measured at the back of the head and loaded end.

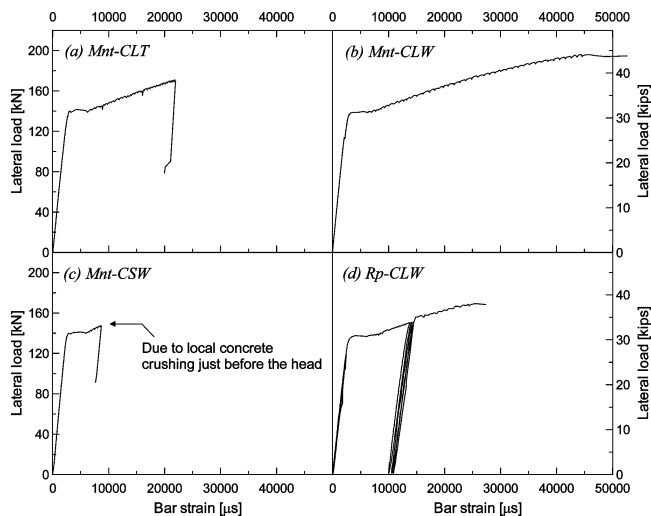


Fig. 10—Bar strains monitored at 50 mm (2 in.) outside the concrete surface under pullout.

headed bars were similar to one another, but quite different from those for nonheaded bars (Mnt-NH series). No brittle concrete breakout was observed for all headed bar specimens, whereas pullout failure occurred for the straight bar anchorage. The headed bar specimens maintained the anchorage strength (by head bearing) even after significant bond deterioration, leading to ductile failure. The bond deterioration was evidenced by a reduction in stiffness of the load-slip relations, and by the observation that the stiffness softening had occurred when splitting cracks began to form.

Results of bar end slips (average: 0.09 and 0.32 mm [0.0035 and 0.0126 in.]) at 70 and 95% of ultimate forces demonstrate satisfactory anchorage behavior for all three head types under monotonic loads, as reported by CEB-FIB Model Code 90<sup>16</sup> (Section 9.1.1.3), which requires them to be within 0.1 and 0.5 mm (0.0039 and 0.0197 in.), respectively. Table 3 indicates that Mnt-CLT (**M**onotonic, **C**ircular **L**arge, **T**hrading) specimens achieved slightly higher anchorage strength (171 kN [38 kips]  $1.28A_s f_{y\_meas}$ ) than that (165 kN [37 kips]  $1.23A_s f_{y\_meas}$ ) obtained for Mnt-CST (**M**onotonic, **C**ircular **S**mall, **T**hrading) or SQT (**M**onotonic, **S**quare, **T**hrading) specimens. This was anticipated because the net bearing areas ( $A_{brg}$ ) of the heads were different.

Figure 8(b) provides similar comparisons for the case where the welded head-to-bar connection was used. Whereas satisfactory anchorage behavior was exhibited for all headed bar specimens, the anchorage strength was particularly increased to 196 kN (44 kips) ( $1.47A_s f_{y\_meas}$ ) for the large head ( $A_{brg}/A_b = 4.5$ ). Due to the strain-hardening at the

welded connection location, it appears that a larger tensile force was transferred (refer to Fig. 10(b) versus 10(a)). The anchorage strengths for the welded and threaded connections were similar for small heads (Table 3).

Similar test results were observed under repeated loading (Fig. 5) and no discrepancies in anchorage behavior (stiffness and strength) between the threaded and welded connections were found for the small head ( $A_{brg}/A_b = 2.6$ ). Measured stresses of all headed bars exceeded the actual yield strength. Particularly, relatively large anchorage strength (179 kN [40 kips]  $1.35A_s f_{y\_meas}$ ) was recorded for the large head. The average bar slips of 0.06 and 0.3 mm (0.0023 and 0.012 in.) at 70 and 95% of the ultimate forces were within tolerable limits of CEB-FIB Model Code 90.<sup>16</sup> The strengths began to degrade at bar slips exceeding 0.5 mm (0.02 in.). The deteriorated anchorage behavior, as compared to that under monotonic tension, is likely due to higher local compressive stresses and associated local concrete damage that often occur when the bar is subjected to repeated loading. This behavior is common for all types of nonlinear anchorages (for example, head or hook versus straight termination), not only for headed anchorages. The test data and post-test observations indicate that concrete eventually crushed at the bearing face of the small head, but a complete concrete breakout failure did not occur. The cone-type failure is typically characterized by a sudden loss of the pullout load to near zero levels right after reaching the peak, which was not seen in any of the load-slip relations.

The results described in the preceding paragraphs are summarized as follows: 1) the net bearing area ( $A_{brg}$ ) of at least 2.6 times the bar area ( $A_b$ ) was effective to maintain bearing resistance even after significant bond deterioration; 2) anchorage strength and behavior under repeated loading were relatively comparable to those under monotonic loading; 3) the head shape did not impact the anchorage condition; and 4) both the threaded and welded head-to-bar connections were effective in transferring the full-design bar force. This conclusion supports the 2004 version of ASTM A970 Specifications,<sup>10</sup> which permit the use of welding, threading, and forging techniques to attach the head to the bar. It is, however, noted that the variation in results would exist if a large number of specimens for each parameter were tested. The results obtained from the pullout tests were used for the selection of head size, shape, and head-to-bar connection (that is, CST) for reversed cyclic testing of headed bars in the beam-column joint.

## CYCLIC TEST RESULTS FOR JOINT SUBASSEMBLIES

### Observed behavior

Observed crack patterns for both JD (headed) and JK (hooked) specimens were similar up to approximately 2.7% drift; however, during 3.5% drift cycles, the extent of joint damage for JK was more apparent than that for JD (Fig. 11(a) versus 11(b)). This might be influenced by different bond qualities, as other conditions were exactly the same. This will be investigated further.

During 0.4% drift cycles, flexural cracks formed on the beam adjacent to the joint. For drift ratios greater than 0.7%, these cracks became significant and were observed up to the midpoint of the beam. Diagonal joint cracks also occurred beyond a drift level of 0.7%. The deterioration of JK was characterized by joint cover spalling and by a gradual accumulation of diagonal strut damage between drift

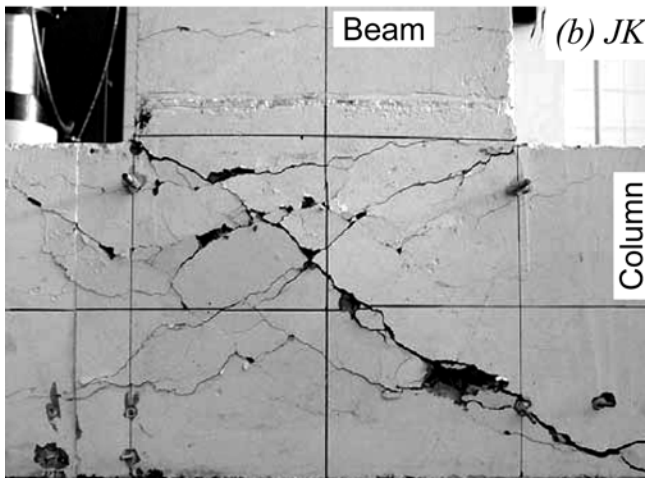
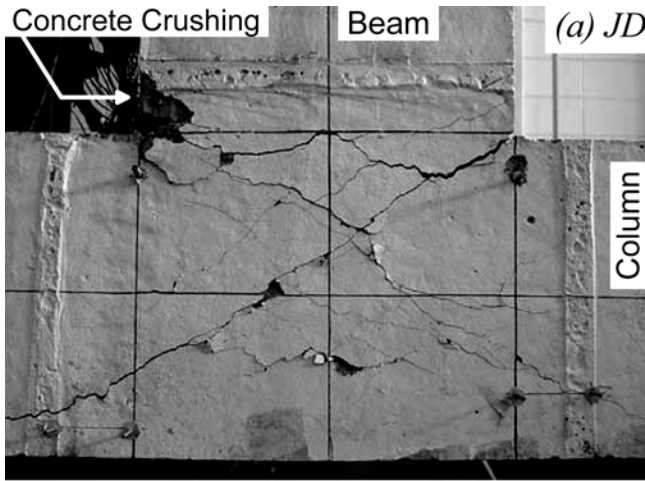


Fig. 11—Observed joint damages at the end of seismic testing.

ratios of 2.7 and 3.5% (Fig. 11(b)). In contrast, JD showed a typical flexural failure of the beam with limited joint deterioration (Fig. 11(a)). Note that this involved full-scale testing and, thus, shear crack widths can be seen more prominently than in other scaled specimens.<sup>17</sup> Significant damage in the diagonal joint strut for JK might be due in part to a relatively moderate degree of joint confinement, which in fact did not adversely affect the overall behavior of JD. The only difference between JD and JK was the anchorage condition; therefore, it is believed that inadequate anchorage of hooked bars might have accelerated the strut failure of the JK specimen at approximately 3% drift. This will be discussed in detail by examining test data in the following subsection.

### Discussion of test data

The relationship of lateral load imposed at the beam end versus story drift is shown in Fig. 12. The lateral load was measured using a load cell mounted on the horizontal actuator located at the beam end (Fig. 7). The drift ratio was taken as the beam end displacement, divided by the distance between the lateral load point and the column center. The peak lateral load ( $L_{peak}$ ), load at first beam yielding ( $L_y$ ), and load at 25% reduction from the peak load ( $L_{0.75peak}$ ) were captured. Also, the corresponding drift ratios ( $\delta_{peak}$ ,  $\delta_y$ , and  $\delta_{0.75peak}$ ) were recorded as listed in Table 5. The backbone envelopes of the loops of the load-drift responses from JD (headed) and JK (hooked) specimens were obtained and compared in Fig. 13.

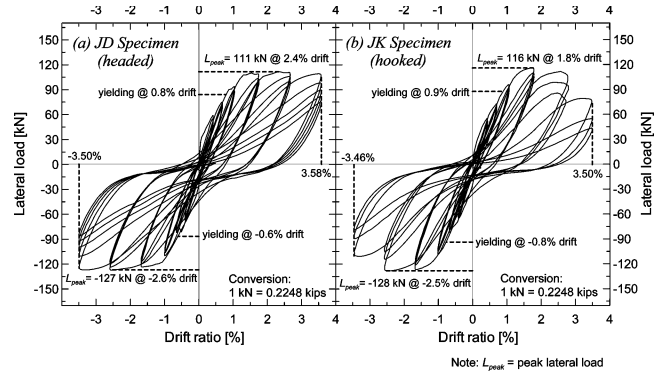


Fig. 12—Lateral load versus drift relations for beam-column joint specimens.

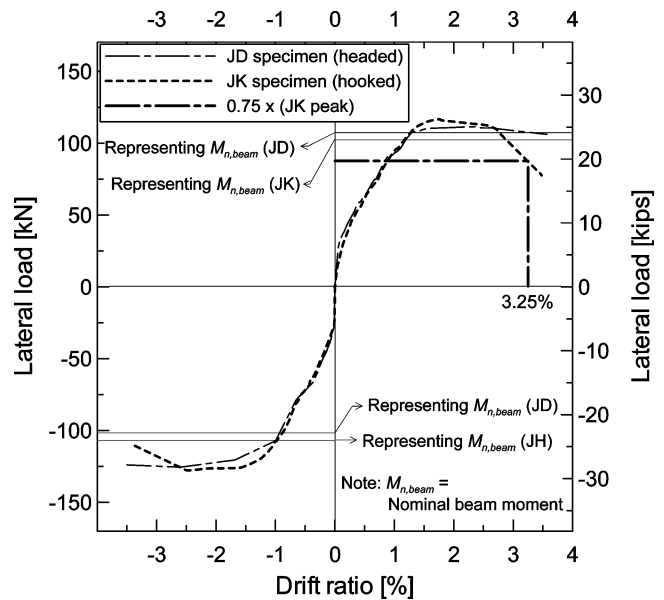


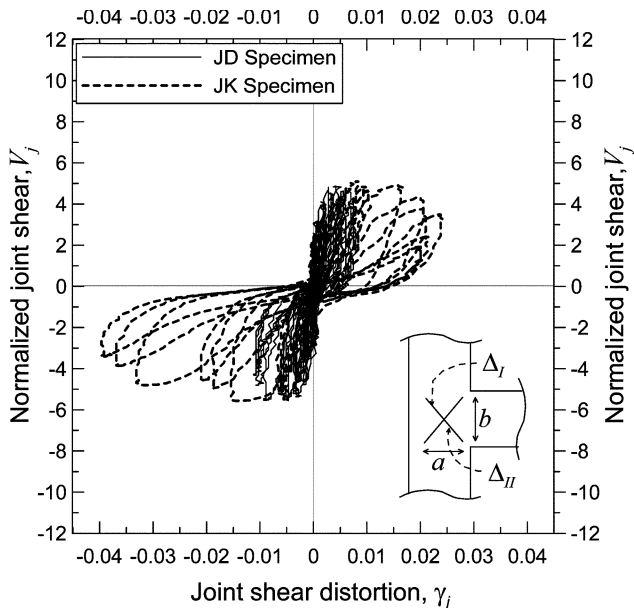
Fig. 13—Backbone envelopes of lateral load-drift relations.

Table 5—Summary of seismic test results

ID		$L_n$ , kN (kips)	$L_{peak}$ , kN (kips)	$\delta_{peak}$ , %	$L_y$ , kN (kips)	$\delta_y$ , %	$\delta_{0.75peak}$ , %
JD (headed)	+	107 (24)	111 (25)	2.36	84 (19)	0.79	NA
	-	107 (24)	127 (29)	2.58	87 (20)	0.61	NA
JK (hooked)	+	102 (23)	116 (26)	1.77	88 (20)	0.90	3.25
	-	102 (23)	128 (29)	2.51	93 (21)	0.77	NA

Note:  $L_n$  corresponds to nominal beam moment capacity.

Figure 12 illustrates that both the JD and JK specimens behaved in a relatively ductile manner, as also evidenced by substantial beam flexural cracking and all tension steel yielding. Based on readings from strain gauges that were attached to beam longitudinal bars at the beam-joint interface, first yielding occurred at approximately 0.6 to 0.9% drifts. This indicates that the embedment depths for both headed and hooked bars were sufficient to develop their yield strengths in the linear range of the load-deformation curve. The lateral stiffness and peak lateral loads were similar for both specimens, exceeding the nominal beam moment strengths  $M_n$  (Fig. 13), where  $M_n$  is calculated using as-measured material properties ( $f'_c = 29.1$  MPa [4.2 ksi] and  $f_{y, meas} = 481$  and 460 MPa [70 and 67 ksi] for JD and JK, respectively).



Note:  $\gamma_j = \frac{(\Delta_I - \Delta_{II})\sqrt{(a^2 + b^2)}}{2ab}$  where  $a$  &  $b$  = avg. of two sides.

$$V_j = \frac{\left[ \frac{\text{Beam moment}}{0.9d} - V_{column} \right]}{0.083\sqrt{f'_c} b h} \text{ (or } \sqrt{f'_c} b h \text{ in lbs.)}$$

Fig. 14—Joint shear versus joint shear distortion relations for JD and JK specimens (refer to References 18 and 19 for calculations of  $\gamma_j$  and  $V_j$ ).

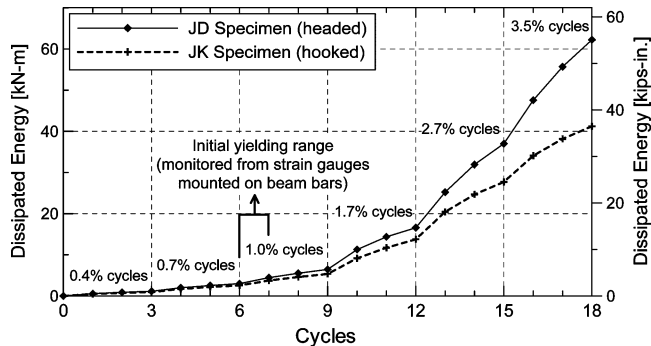


Fig. 15—Cumulative external work for JD and JK specimens.

The peak lateral loads were reached at drifts of approximately 2 to 2.5% and maintained until about 3.5% drift for JD, whereas for JK, after reaching the peak the lateral load, subsequently dropped to 75% of the peak at +3.25% drift (Fig. 13). ACI 374.1-05<sup>15</sup> defines the failure criterion as a drop to 75% of the peak lateral load. Therefore, the performance of JK specimen did not meet ACI 374.1-05<sup>15</sup> criteria that the failure should be precluded at drift ratios less than 3.5%.

Two potential reasons might exist for the relatively poor seismic performance noted from the JK testing: 1) insufficient development length of the hooked bar; and 2) moderate joint confinement. Even though the edge of the hooked bar was not located (133 mm [5.2 in.]) within 51 mm (2 in.) from the outside of the joint core (as recommended by ACI 352R-02,<sup>5</sup> Section 4.5.2.1), it appears that the bend of the hooked bar was still located inside the main diagonal strut (refer to Fig 1(b)).

Table 6—Comparisons between test results and ACI 374.1-05<sup>15</sup> acceptance criteria

ID	$\delta$ at $M_n$ , %	$M_{peak}/M_n$	During third cycle of 3.5% drift cycles			
			$M_{3rd}/M_{peak}$	$\beta$	$K_s/K$	$K'_s/K'$
(1)	(2)	(3)	(4)	(5)	(6)	(7)
Acceptance criteria	$\leq 2\%$	$\leq 1.25$	$\geq 0.75$	$\geq 0.125$	$\geq 0.05$	$\geq 0.05$
JD (+)	1.3	1.09	0.77	0.233	0.117	0.072
JD (-)	1.0	1.19	0.77			
JK (+)	1.2	1.10	0.36	0.158	0.042	0.037
JK (-)	0.9	1.25	0.61			

Note:  $\delta$  at  $M_n$  is drift ratio at which  $M_n$  is reached;  $M_n$  is nominal moment (based on design material properties);  $M_{peak}$  is peak moment (measured);  $M_{3rd}$  is peak moment during third cycle of 3.5% drift (measured);  $\beta$  is relative energy dissipation ratio (ACI 374.1-05<sup>15</sup>);  $K_s$  is secant stiffness from -0.35% to +0.35% drift during third cycle of 3.5% drift ratio;  $K'_s$  is secant stiffness from 0.35% to -0.35% drift during third cycle of 3.5% drift ratio;  $K$  is initial stiffness for positive bending; and  $K'$  is initial stiffness for negative bending.

That is based on the observation that the performance of JD (headed) with the same embedment depth was still satisfactory (refer to Table 6). As mentioned previously, the hooked bars were provided with a shorter development length than  $l_{dh}$ . This adversely affected the anchorage behavior in the nonlinear range of deformation, particularly beyond a 2.5% drift ratio (Fig. 12). On the other hand, the JD test results indicate that the embedment length of  $15d_b$  ( $0.17f_{y\_meas}d_b/\sqrt{f'_{c\_meas}}$ ) was sufficient for headed bars with small heads ( $A_{brg}/A_b = 2.6$ ). This is solely based on the fact that the performance of JD generally met the ACI 374.1-05<sup>15</sup> criteria, particularly pinching indexes (refer to Columns (6) and (7) of Table 6).

The lack of joint confinement (Type 1 detailing) eventually resulted in joint shear failure at a drift of 2.5 to 3% in conjunction with poorer anchorage behavior for JK (versus JD). It is interesting to note that even with the same conditions, JD (headed) experienced no loss of the lateral load capacity until the end of testing (up to 3.5% drift [Fig. 12]). Moreover, modest joint shear distortions (average of maximum for both drifts  $\leq 0.01$ ) were monitored (refer to Fig. 14). As such, the lack of joint confinement did not pose a serious problem for the beam-column joint with headed bars. This is an interesting aspect, as it implies the possibility for the reduction of joint transverse reinforcement when utilizing headed bars as beam longitudinal reinforcement. The bearing stresses acting against the head are considered to be partially transferred to column lateral reinforcement and (confined) column concrete above the joint by external truss action, as shown in Fig. 1(a). Although joint shear distortion data, in part, support this action, it would have been better to monitor strains in column and joint transverse reinforcement (only longitudinal reinforcement was measured in this test). A potential for the reduction of joint reinforcement when using headed bars warrants further investigation with more data.

Due to the limitation of the actuator stroke, the drift ratio could not be increased further. Instead, two more cycles were repeated at 3.5% drift for the JD specimen. At the third and fifth cycles of 3.5% drift, peak lateral loads were reduced by 17 and 30% of the first cycle peak load, respectively (Fig. 12). The 17% reduction for the third cycle at 3.5% drift meets the ACI 374 acceptance criteria, and the 30% reduction at the fifth cycle can be considered not critical. All other

acceptance criteria of ACI 374.1-05<sup>15</sup> were satisfied as indicated in Table 6.

Figure 15 displays a comparison of the energy dissipated during the drift cycles, indicating that the hysteretic energy dissipated at each drift level for JD was substantially larger than JK. The better energy dissipation capacity after initial yielding for JD indicates the improved anchorage behavior of headed bars under inelastic deformation reversals for the given development length. The apparent degree of pinching shown in Fig. 12(a) versus 12(b) is also consistent with this behavior. The energy dissipation capacity of reinforced concrete beams is one of the key design aspects of ductile moment frames. Based on the results described in this and in the previous paragraphs, it is concluded that use of headed bars, with  $l_p$  of  $15d_b$  ( $0.17f_{y, meas}d_b/\sqrt{f'_{c, meas}}$ ) and ( $A_{brg}/A_b$ ) of 2.6, was effective in transferring the beam moment to the exterior column without loss up to 3.5% drift. Additionally, the tests showed that shorter development length for headed bars was sufficient compared with hooked bars, claiming different required development lengths between headed and hooked bars (and supporting ACI 352R-02,<sup>5</sup> and ACI 318-08<sup>1</sup> Sections 12.1 and 12.6). Finally, the seismic test results support that Eq. (2) or (3), which is shorter than Eq. (1), works well for estimating development length of a headed bar in a Type 1 or Type 2 beam-column joint.

### Relationship of new ACI 318 provisions for headed bars and test results

Although the joint specimen was constructed before new ACI 318 provisions for headed bars were added, it is worth evaluating the performance using the new ACI 318 code.<sup>1</sup> As concluded in the preceding sections, the ACI 318 specified development length (Eq. (1)), along with head size ( $A_{brg}/A_b$ ) of approximately 3, ensures satisfactory anchorage/bond behavior of headed bars anchored in exterior beam-column joints. The results herein are of value, as they validate the new ACI 318-08 provision. Based on the results, the head size of ( $A_{brg}/A_b$ ) of 3 could even be acceptable for headed bars in beam-column joints. Additional cyclic tests, however, would be useful to verify this finding.

Material properties used for the tests were within the limitations set forth by ACI 318-08 (Sections 12.6.1 and 12.6.2). The clear cover to the bar ( $c_{cb}$ ; refer to Fig. 2) and the clear bar spacing ( $c_s$ ; refer to Fig. 2) tested were  $3.6d_b$  and  $4.2d_b$ , respectively. These values are greater than the required minimum values of  $2d_b$  and  $4d_b$ , respectively, and would not produce any adverse effects on seismic performance of the exterior beam-column joint. Additional research would be needed to assess current restrictions on such parameters, particularly on headed bar clear spacing. The spacing of  $4d_b$  is rather limiting and may not be ideal for the industry. From this study, the head thickness ( $t_{head}$ ; refer to Fig. 2) of at least  $1d_b$  appears reasonable to ensure effective head bearing with little deformation in the steel. There are currently no provisions on head thickness in ACI 318-08.

### SUMMARY AND CONCLUSIONS

Pullout and seismic tests were conducted to investigate the applicability of headed bars with small heads. The test data were assessed to examine the effects of the head size, shape, and head-attaching technique on the anchorage behavior under both monotonic and repeated loads. The results from full-scale seismic testing of a joint with headed bars were evaluated by comparison with a companion specimen with

hooked bars and by using the acceptance criteria of ACI 374.1-05.<sup>15</sup> Based on the test results, the following conclusions were reached.

1. No brittle concrete breakout occurred for any headed bars in pullout, provided that the head size ( $A_{brg}/A_b$ ) was at least 2.6 and the embedment depth was  $10d_b$  ( $0.13f_{y, meas}d_b/\sqrt{f'_{c, meas}}$ ).

2. The loading condition (monotonic versus repeated), head shape (circular versus square), and head-attaching technique (threading versus welding) did not influence the anchorage behavior substantially during pullout. These results are consistent with ASTM A970-04<sup>10</sup> and ACI 318-08<sup>1</sup> (Section 3.5.9).

3. The headed bars with large heads ( $A_{brg}/A_b = 4.5$ ) exhibited higher anchorage strengths than the headed bars with small heads ( $A_{brg}/A_b = 2.6$  to 2.8).

4. The test results of the joint subassemblies support the applicability of headed bars with small heads ( $A_{brg}/A_b = 2.6$ ) in exterior beam-column joints and the new ACI 318-08<sup>1</sup> provision on headed bars (Section 12.6).

5. The exterior joint containing headed bars with a development length of  $15d_b$  (or  $0.17f_{y, meas}d_b/\sqrt{f'_{c, meas}}$ ) and with head size ( $A_{brg}/A_b$ ) of approximately 3 was capable of transferring probable moments and forces in the members without loss up to 3.5% drift, and generally met ACI 374.1-05<sup>15</sup> acceptance criteria. On the other hand, the joint with hooked bars did not meet acceptance criteria.

6. The aforementioned performance was achieved even with moderate (Type 1) joint confinement. The satisfactory seismic performance, such as suppressed joint shear deformations, indicate that reduced joint confinement does not influence adversely on the headed bar anchorage in the interstory joints, likely due to the different bearing stress-transfer path provided by the external truss formed above the joint. This implies a possibility that the amount of transverse reinforcement in the exterior interstory joint may be reduced when headed bars are utilized (versus hooked bars).

### ACKNOWLEDGMENTS

The work presented in this paper was a part of the research results for the Korea Research Foundation under Grant No. KRF-2005-050-D0017, and the U.S. part of the research was supported by the Oklahoma Transportation Center (OTCREOS9.1-27). The testing was conducted at the laboratory of Hankyong National University, Ansong, Korea. The authors would like to acknowledge W. Kim, a PhD student, University of Oklahoma, Norman, OK, for his assistance and H.-J. Lee, an Assistant Professor, National Yunlin University of Science and Technology, Taiwan, for his helpful discussion. The views expressed are those of authors and do not necessarily represent those of the sponsors.

### REFERENCES

1. ACI Committee 318, "Building Code Requirements for Structural Concrete (ACI 318-08) and Commentary," American Concrete Institute, Farmington Hills, MI, 2008, 473 pp.
2. DeVries, R. A.; Jirsa, J. O.; and Bashandy, T., "Anchorage Capacity in Concrete of Headed Reinforcement with Shallow Embedments," *ACI Structural Journal*, V. 96, No. 5, Sept.-Oct. 1999, pp. 728-737.
3. Park, H. K.; Yoon, Y. S.; and Kim, Y. H., "The Effect of Head Plate Details on the Pull-Out Behaviour of Headed Bars," *Magazine of Concrete Research*, V. 55, No. 6, Dec. 2003, pp. 485-496.
4. Thompson, M. K.; Ziehl, M. J.; Jirsa, J. O.; and Breen, J. E., "CCT Nodes Anchored by Headed Bars—Part 1: Behavior of Nodes," *ACI Structural Journal*, V. 102, No. 6, Nov.-Dec. 2005, pp. 808-815.
5. Joint ACI-ASCE Committee 352, "Recommendations for Design of Beam-Column Connections in Monolithic Reinforced Concrete Structures (ACI 352R-02)," American Concrete Institute, Farmington Hills, MI, 2002, 37 pp.
6. Wright, J. L., and McCabe, S. L., "The Development Length and Anchorage Behavior of Headed Reinforcing Bars," *SM Report* No. 44,

Structural Engineering and Engineering Materials, University of Kansas, Center for Research, Lawrence, KS, Sept., 1997, 147 pp.

7. Wallace, J. W.; McConnell, S. W.; Gupta, P.; and Cote, P. A., "Use of Headed Reinforcement in Beam-Column Joints Subjected to Earthquake Loads," *ACI Structural Journal*, V. 95, No. 5, Sept.-Oct. 1998, pp. 590-606.

8. Chun, S. C.; Lee, S. H.; Kang, T. H.-K.; Oh, B.; and Wallace, J. W., "Mechanical Anchorage in Exterior Beam-Column Joints Subjected to Cyclic Loading," *ACI Structural Journal*, V. 104, No. 1, Jan.-Feb. 2007, pp. 102-113.

9. ASTM A970/A 970M-98, "Standard Specification for Welded or Forged Headed Bars for Concrete Reinforcement," ASTM International, West Conshohocken, PA, 1998, 7 pp.

10. ASTM A970/A 970M-04a, "Standard Specification for Headed Steel Bars for Concrete Reinforcement," ASTM International, West Conshohocken, PA, 2004, 8 pp.

11. Choi, D.-U., "Test of Headed Reinforcement in Pullout 2: Deep Embedment," *KCI Concrete Journal*, V. 18, No. 3E, Dec. 2006, pp. 151-159.

12. Choi, D.-U.; Hong, S. G.; and Lee, C. Y., "Test of Headed Reinforcement in Pullout," *KCI Concrete Journal*, V. 14, No. 3, Sept. 2002, pp. 102-110.

13. Korea Concrete Institute, "Design Code for Concrete Structures

(KCI-03)," Korea Concrete Institute, Seoul, Korea, 2003, 405 pp. (in Korean)

14. Meinheit, D. F., and Jirsa, J. O., "Shear Strength of R/C Beam-Column Connections," *Journal of the Structural Division*, ASCE, V. 7, No. ST11, Nov. 1981, pp. 2227-2244.

15. ACI Committee 374, "Acceptance Criteria for Moment Frames Based on Structural Testing and Commentary (ACI 374.1-05)," American Concrete Institute, Farmington Hills, MI, 2005, 9 pp.

16. Comité Euro-International du Béton, Lausanne, "CEB-FIB Model Code 1990 (CEB-FIB MC 90)," Thomas Telford Services Ltd., London, UK, 1993, 437 pp.

17. Chung, L., and Shah, S. P., "Effect of Loading Rate on Anchorage Bond and Beam-Column Joints," *ACI Structural Journal*, V. 86, No. 2, Mar.-Apr. 1989, pp. 132-142.

18. Paulay, T., "Equilibrium Criteria for Reinforced Concrete Beam-Column Joints," *ACI Structural Journal*, V. 86, No. 6, Nov.-Dec. 1989, pp. 635-643.

19. Siohara, H., "New Model for Shear Failure of RC Interior Beam-Column Connections," *Journal of Structural Engineering*, ASCE, V. 127, No. 2, Feb. 2001, pp. 152-160.